Requirement for *Lmo4* in the Vestibular Morphogenesis of Mouse Inner Ear

Min Deng[1], **Ling Pan**[1], **Xiaoling Xie**[1], and **Lin Gan**[1,2,3,*]

[1]University of Rochester Eye Institute, University of Rochester, Rochester, NY 14642

[2]Center for Neural Development and Disease, University of Rochester, Rochester, NY 14642

[3]Department of Neurobiology and Anatomy, University of Rochester, Rochester, NY 14642

Abstract

During development, compartmentalization of an early embryonic structure produces blocks of cells with distinct properties and developmental potentials. The auditory and vestibular components of vertebrate inner ears are derived from defined compartments within the otocyst during embryogenesis. The vestibular apparatus, including three semicircular canals, saccule, utricle, and their associated sensory organs, detects angular and linear acceleration of the head and relays the information through vestibular neurons to vestibular nuclei in the brainstem. How the early developmental events manifest vestibular structures at the molecular level is largely unknown. Here, we show that LMO4, a LIM-domain-only transcriptional regulator, is required for the formation of semicircular canals and their associated sensory cristae. Targeted disruption of *Lmo4* resulted in the dysmorphogenesis of the vestibule and in the absence of three semicircular canals, anterior and posterior cristae. In *Lmo4*-null otocysts, canal outpouches failed to form and cell proliferation was reduced in the dorsolateral region. Expression analysis of the known otic markers showed that *Lmo4* is essential for the normal expression of *Bmp4*, *Fgf10*, *Msx1, Isl1, Gata3*, and *Dlx5* in the dorsolateral domain of the otocyst, whereas the initial compartmentalization of the otocyst remains unaffected. Our results demonstrate that *Lmo4* controls the development of the dorsolateral otocyst into semicircular canals and cristae through two distinct mechanisms: regulating the expression of otic specific genes and stimulating the proliferation of the dorsolateral part of the otocyst.

Keywords

Introduction

The compartmentalization process plays an important role in the development of the vertebrate nervous systems. In the developing central nervous system (CNS), the cytologically homogeneous sheet of neural epithelial cells is initially partitioned along the anterior-posterior axis into regions representing the anlagen of forebrain, midbrain, hindbrain, and the spinal cord in the posterior (Lumsden and Krumlauf, 1996). Within each region, neuronal cell types are generated with unique identities assessed by morphology, physiological properties, and axon projections. Moreover, each of these regions is further patterned into distinct subregions such

*Corresponding author. lin_gan@urmc.rochester.edu, phone: (585)273-1510, FAX: (585)276-2432..

that in the forebrain, compartments are formed to develop into unique functional regions processing cognitive, motor, and sensory information (O'Leary and Nakagawa, 2002).

The compartmentalization process is similarly important in the development of the peripheral nervous system. The mammalian inner ear is a complex structure containing two functional parts, cochlea and vestibule. The cochlea is a coiled structure and is responsible for auditory function. The vestibular system consists of a central vestibule, three semicircular canals, and an endolymphatic duct and sac. It is essential for balance by sensing gravity, linear and rotational motion. The entire inner ear structure is derived from the otic placode, a thickening ectoderm near the hindbrain (Fritzsch et al., 2002). Previous grafting and lineage tracing experiments in chick embryos have demonstrated that specific parts of the inner ear are derived from distinct compartments of the early otocyst (Baker and Bronner-Fraser, 2001; Fekete, 1996). While the cochlea arises from a ventrally extending region of the ventral otocyst, vestibular structures develop from the dorsolateral otocyst and the endolymphatic duct and sac come from the small dorsomedial projection of the otocyst (Morsli et al., 1998). Recent fate mapping experiments in chicken otic placodes have shown that otic neurons and their sensory targets come from a common proneural domain, in which different precursors are spatially segregated. The otic placode is spatially partitioned along the dorsal/ventral axis with dorsal (cristae) located in the anterior and lateral domain, ventral (cochlea) in the posterior and medial region, and the maculae in an intermediate position (Bell et al., 2008). These otic compartments are demarcated early by the expression of specific regulatory genes, namely the otic patterning genes (Bober et al., 2003; Fekete, 1996). Genetic alteration of the otic patterning genes often leads to defective morphogenesis of the inner ear. For example, the paired-class homeobox gene, *Pax2*, is mostly expressed in the medioventral part of the otocyst. Inactivation of *Pax2* in mice resulted in either agenesis or severe malformation of the cochlea whereas the development of the vestibule is unaffected (Burton et al., 2004; Torres et al., 1996). The *Hmx* homeobox genes, *Hmx2* and *Hmx3* (*Nkx5.2* and *Nkx5.1*, respectively), are co-expressed in the dorsolateral otic epithelium (Wang et al., 2001; Wang et al., 2004b). Targeted disruption of *Hmx2* results in agenesis of all semicircular canals and a severe loss in the three cristae and the macula utriculus (Wang et al., 2001). A null mutation in *Hmx3* causes a significant loss of sensory cells in the fused utriculosaccular cavity and an absence of the lateral crista (Wang et al., 1998). A compound null mutation of *Hmx2* and *Hmx3* results in a complete loss of the entire vestibular structures, demonstrating their redundant and distinct role in vestibular development (Wang et al., 2004b). The *distal-less* class homeobox gene, *Dlx5* and *Dlx6*, are expressed in the dorsal otic epithelium and mice deficient for these two genes fail to form dorsal otic derivatives including the semicircular ducts, utricle, saccule, and endolymphatic duct (Acampora et al., 1999; Merlo et al., 2002). Despite our knowledge about the contribution of these transcription factors in establishing patterns of growth and differentiation within distinct otocyst compartments, the regulatory relationship among these factors is not fully understood.

In addition to transcription factors, signaling pathways are critical in the induction of the otic placode and in the subsequent morphogenesis of the otocyst. The mesenchymal fibroblast growth factors, FGF8 and FGF10, are required together with FGF3 from hindbrain for the expression of otic placode genes and for otic placode induction and vesicle formation (Adamska et al., 2001; Alvarez et al., 2003; Hatch et al., 2007; Ladher et al., 2005; Wright and Mansour, 2003a; Wright and Mansour, 2003b; Zelarayan et al., 2007). WNT signals from the hindbrain are necessary to limit the region of ectoderm that forms the otic placode and are sufficient to maintain the expression of dorsal otic genes (Ohyama et al., 2006; Riccomagno et al., 2005). WNT1 and WNT3a from the dorsal hindbrain are required redundantly for the formation of the vestibular structures (Riccomagno et al., 2005). FGF3 prevents the ventral expansion of WNT3a and restricts WNT signals on the dorsal otocyst (Hatch et al., 2007). Sonic hedgehog (SHH) secreted from the notochord is required for the specification of ventral otic fate (Bok et al., 2007; Riccomagno et al., 2002). The restricted expression of WNT target

genes to the dorsal otocyst is also influenced by SHH (Riccomagno et al., 2005). Thus, a balance between FGF/WNT (dorsal) and SHH (ventral) signaling activities is important in determining the vestibular and auditory cell types. FGF signals are also important for otocyst morphogenesis. Gain- and loss-of-function experiments show that FGFs in the sensory cristae promote non-sensory canal development by upregulating *Bmp2* (Chang et al., 2004). Studies in chickens and mice have shown that the formation of semicircular canals and their cristae requires BMP signals (Chang et al., 2008; Chang et al., 1999; Gerlach et al., 2000).

Here, we show that targeted disruption of *Lmo4*, a nuclear LIM-domain-only transcription regulator, results in a profound defect in the vestibular system of mouse inner ears including the absence of three semicircular canals, anterior and posterior cristae. Without *Lmo4*, canal outpouches fail to form and cell proliferation is significantly reduced in the dorsolateral otocyst. Interestingly, loss of *Lmo4* does not affect the initial compartmentalization of the otocyst. Rather, *Lmo4* is required for the normal expression of *Bmp4*, *Fgf10*, *Msx1, Isl1, Gata3*, and *Dlx5* in the dorsolateral otic vesicle. Our results demonstrate that *Lmo4* plays an essential role in vestibular morphogenesis by regulating cell proliferation and maintaining otic gene expression in the dorsolateral otocyst.

Materials and methods

Generation of Lmo4-null mice

The *Lmo4-lacZ* (*Lmo4^lacZ^*) knock-in mutation was generated by inserting the *Lmo4* 4.3 kb 5′- and 3.0 kb 3′-flanking sequences into the 5′ and 3′ multiple cloning sites of pKII-*lacZ* knock-in vector (L. G., unpublished), respectively. In *Lmo4^lacZ^* knock-in construct, the coding region of Exon 2 and a part of Intron 2 were replaced by *lacZ* reporter gene and SV40 polyA sequences (Fig. 1A). The construct placed *lacZ* under the control of *Lmo4* regulatory sequences and allowed the study of *Lmo4* expression. *Lmo4^lacZ^* knock-in construct was linearized by *NotI*–digestion and introduced into W4 embryonic stem (ES) cells by electroporation (Auerbach et al., 2000). We obtained 11 targeted ES clones from 192 G418-resistant clones screened by Southern blot analysis and generated *Lmo4^lacZ^* knock-in mice from two targeted ES cell clones. To generate *Lmo4* conditional knockout allele (*Lmo4^cko^*), we created the targeting construct by using two loxP sequences to flank Exon 2 (Fig. 1B). After electroporation of W4 ES cells with *Lmo4^cko^* construct, we obtained 2 positive ES clones from 144 G418-resistant clones by Southern blot screening. Both targeted ES clones were used to generate the *Lmo4^cko^* mice. The FRT-flanked neomycin resistance gene in *Lmo4^cko^* mice was removed by crossing *Lmo4^cko^* mice with ROSA26-FLPe mice (The Jackson Laboratory, Stock Number: 003946) to generate heterozygous *Lmo4^lox/+^* mice. We then crossed *Lmo4^lox/+^* with tissue-specific *Foxg1^Cre^* deleter mice (Hebert and McConnell, 2000) to remove *Lmo4* specifically in the inner ear (Fig. 1B). Southern genotyping confirmation of *Lmo4^lacZ^*, *Lmo4^cko^*, and *Lmo4^lox^* alleles was performed by using a 3′-probe on *EcoRI*-digested genomic DNA to detect 3.8, 9.8, and 6.7 kb fragments in wild type, *Lmo4^lacZ^*, and *Lmo4^lox^* mice, respectively (Fig. 1C). Additionally, PCR methods were used to genotype mice from subsequent breeding of *Lmo4^lacZ^* mice. The PCR primers used to identify wild type *Lmo4* allele were 5′-TGCCGGCGAGCCTCCCTTCTTC-3′ and 5′-GGCAGCCCGACTTACCTA-3′, and *Lmo4^lacZ^* allele 5′-AGGGCCGCAAGAAAACTATCC-3′ and 5′-ACTTCGGCACCTTACGCTTCTTCT-3′. All analyses were done on a mixed C57BL/6J and 129S6 background. Embryos were identified as E0.5 at noon on the day at which vaginal plugs were observed. The University Committee of Animal Resources (UCAR) at University of Rochester approved all animal procedures used in this study.

Paint-filling analysis

Paint-fill injections were performed as described (Morsli et al., 1998). Briefly, mouse embryos at E11.5 to E15.5 were harvested and fixed overnight in Bodian's fixative. Embryos were then dehydrated in ethanol and cleared in methyl salicylate. The inner ears were visualized by injecting 0.1% white latex paint in methyl salicylate into the membranous labyrinth. At E11.5, the injection micropipette was inserted in the lateral surface of the otocyst. For E15.5 inner ears, latex paint was injected into the cochlea. Five or more inner ears were injected for each stage examined.

Immunohistochemistry, BrdU labeling, X-Gal staining, and in situ hybridization

For immunolabeling, cryosections were cut at a thickness of 14 μm. Primary antibodies and concentrations used for this study were: mouse anti-bromodeoxyuridine (BrdU) (Becton Dickson, 1:200), rabbit anti-Caspase3 (R&D system, 1:500), goat anti-LMO4 (Santa Cruz, 1:200), rabbit polyclonal anti-Pax2 (Covance, 1:200) and mouse anti-b-Tubulin (TuJ1) (Covance, 1:500). Alexa-conjugated secondary antibodies were obtained from Molecular Probes, Inc. and were used at a concentration of 1:1,000. Images were captured with a Zeiss 510 META confocal microscope.

Detection of β-galactosidase activity was determined by X-Gal staining (Gan et al., 1999). Briefly, embryos were fixed in 4% paraformaldehyde in PBS at 4°C for 30 minutes. Whole-mount embryos or 20 μm frozen sections were stained overnight at room temperature with 0.1% X-Gal, 5 mM potassium ferricyanide, 5 mM potassium ferrocyanide, 2 mM $MgCl_2$ in PBS. For bromodeoxyuridine (BrdU) (Sigma) pulse-labeling experiments, pregnant females were injected intraperitoneally with 100 μg BrdU/gram body weight one hour before they were sacrificed. Embryo processing and anti-BrdU labeling were performed on serial sections as previously described (Mishina et al., 1995).

For whole-mount and section in situ hybridization, embryos were dissected in phosphate-buffered saline (PBS), fixed in 4% paraformaldehyde in PBS, and subjected to whole-mount in situ hybridization as previously described (Wilkinson, 1992). For section in situ hybridization, embryos were embedded and frozen in OCT medium (Tissue-Tek), sectioned at 20 μm thickness. Hybridization was carried out with specific digoxigenin-labeled RNA probes and detection was done with anti-CIP/NBT color development as previously described (Li and Joyner, 2001).

Results

Targeted disruption of Lmo4

To investigate the role of *Lmo4* during inner ear development, we have generated two targeted deletion alleles of *Lmo4*, *Lmo4-lacZ* (*Lmo4^{lacZ}*) knock-in and *Lmo4* conditional knockout (*Lmo4^{lox}*), by homologous recombination (Figs. 1A-C). To confirm the targeted disruption, we used anti-LMO4 immunolabeling and detected no expression of LMO4 in *Lmo4$^{lacZ/lacZ}$* homozygous mutant embryos and an absence of LMO4 in otic epithelial cells but not in the peri-otic mesenchymal cells of *Lmo4* inner-ear-specific knockout (*Lmo4$^{lox/lox}$*; *Foxg1^{Cre}* or *Lmo4$^{lox/lacZ}$*; *Foxg1^{Cre}*) mice at E10.5 (Fig. 1D). *Lmo4$^{lacZ/+}$* heterozygous mice were fertile and appeared normal with no overt defects. However, consistent with the phenotypes previously reported in *Lmo4*-null mice (Hahm et al., 2004; Lee et al., 2005; Tse et al., 2004), homozygous *Lmo4$^{lacZ/lacZ}$* mutants died at birth and approximately 30% (n=30 out of 98) of *Lmo4$^{lacZ/lacZ}$* embryos were defective in neural tube closure (exencephaly), in which the cranium is absent and the brain is exposed (Fig. S1). Not surprisingly, *Lmo4* inner-ear-specific knockout mice exhibited no defects in neural tube closure or exencephaly (data not shown).

Compartmentalized expression of Lmo4 in the early otocyst

We first detailed the spatiotemporal expression pattern of *Lmo4* during the early development of mouse inner ear using in situ hybridization. Compared with *Dlx5* expression in the surface ectoderm at the time of otic placode induction at E8 (8-10 somites), *Lmo4* expression was first detected in the mesenchymal cells underneath the surface ectoderm. Subsequently, *Lmo4* expression was observed in the otic placode along with the expression in the mesenchymal cells by the completion of otic induction at E8.5 (12 somites) (Figs. 2A-D). Later, *Lmo4* expression becomes restricted in the lateral region of the posterior otocyst at E9.5 and in the dorsolateral otocyst at E10.5 (Figs. 2E-H, S2). The compartmentalized expression of *Lmo4* in the early otocyst suggests a role in the vestibular genesis.

To study the effect of *Lmo4*-null mutation on *Lmo4*-expressing region in the developing otocyst, we analyzed the expression of *Lmo4*-lacZ knock-in reporter during the early stages of otic development in $Lmo4^{lacZ/+}$ and $Lmo4^{lacZ/lacZ}$ embryos by whole-mount X-Gal staining for β-galactosidase activity. Consistent with *Lmo4* mRNA expression (Fig. 2E), *Lmo4*-lacZ was expressed in the lateral region of the posterior otocyst at E9.5 (Figs. 2I, K). At this stage, lacZ expression in $Lmo4^{lacZ/lacZ}$ otocysts appeared to be normal (Figs. 2J, L; n=8). At E10, *Lmo4*-lacZ expression domain became a more defined band in the dorsolateral otocyst (Figs. 2M, O), a region essential for the development of the three semicircular apparatus (Wang et al., 2004b). There, *Lmo4*-lacZ was expressed in two distinct patches, an anterior domain and a posterior focus (Figs. 2M, O; arrows and arrowheads, respectively). The *Lmo4* expression domain overlapped with the expression domain of *Bmp4*, a marker of the presumptive cristae (Deng et al., 2006;Morsli et al., 1998) and was adjacent to that of *Lfng* (Figs. 2G, H), an early marker for the macula utriculi, the macula sacculi and the cochlea (Morsli et al., 1998). In the $Lmo4^{lacZ/lacZ}$ otocyst, the *Lmo4*-lacZ expression domain in the posterior otocyst at E10 was significantly reduced and the mutant otocysts were smaller (Figs. 2N, P; arrows and arrowheads; n=6). Subsequently at E11.5, when the anterior and posterior semicircular canals began to develop, *Lmo4*-lacZ activity was detected strongly in two newly formed epithelial semicircular ducts in $Lmo4^{lacZ/+}$ embryos (Fig. 2S; arrows). However, no identifiable semicircular duct was seen in the *Lmo4*-null inner ear though residual lacZ activity was detected in a small domain of the $Lmo4^{lacZ/lacZ}$ inner ear (Fig. 2T; arrowhead; n=6). At E12.5, when lateral semicircular ducts started to form, *Lmo4*-lacZ expression revealed three developing semicircular canals in control embryos (Figs. 2Q, U; arrows). In contrast, these canal structures were absent in $Lmo4^{lacZ/lacZ}$ and lacZ expression was only detected in the rudimentary structures in the middle portion of the mutant inner ear (Figs. 2R, V; arrowheads; n=9), demonstrating the absence of semicircular canal formation in *Lmo4*-null inner ears.

Absence of Semicircular Canals in the Lmo4-null Inner Ear

To evaluate further the gross anatomy of *Lmo4*-null inner ears, we used the paint-fill technique at E15.5, a stage when the membranous labyrinth of the inner ear nearly completes its complex morphogenesis and achieves the mature structure (Morsli et al., 1998). In contrast to wild type controls that contain a coiled cochlear duct and a vestibule of three semicircular canals, utricle and saccule, *Lmo4*-null inner ears, with or without the neural tube closure defect, lacked all three semicircular canals and the anterior and posterior ampullae that house the sensory cristae. Interestingly, the lateral ampullae, the utricle and saccule were present in *Lmo4*-null ears (Fig. 3A). Moreover, the endolymphatic duct of the *Lmo4*-null embryo was slightly broader than that of the littermate control. At this stage, whereas the control cochlea completes one and one-half turns (Morsli et al., 1998), The *Lmo4*-null cochlea was shorter and had only one and one-quarter turns (Fig. 3A; inserts).

The early expression of *Lmo4* in both the otocyst and the surrounding mesenchymal cells prompted us to test whether the inner ear-specific removal of *Lmo4* might result in the same

vestibular defect observed in the *Lmo4* conventional knockout. An analysis of paint-filled inner ears of *Lmo4^{lox/lox}; Foxg1^{Cre}* or*Lmo4^{lox/lacZ}; Foxg1^{Cre}* mice demonstrated that these *Lmo4^{null}* inner ears (n=5) exhibited vestibular defects identical to those of *Lmo4^{lacZ/lacZ}* embryos (n=14) at E15.5 (Fig. 3A). Thus, the inner ear-specific deletion of *Lmo4* results in similar vestibular defects to those observed in *Lmo4*-null mice. Furthermore, the lack of neural tube closure defect in *Lmo4* inner ear-specific knockout and 70% of *Lmo4^{lacZ/lacZ}* mice (compare Figs. 2T and V) also confirmed that the vestibular defect was not an indirect effect resulting from a failure in neural tube closure. X-Gal staining of the inner ear sections from these three *Lmo4*-deficient mice revealed an identical phenotype in that they all contained the macula utriculi, the macula sacculi, the lateral crista and the cochlea, but lack the three semicircular canals and anterior and posterior cristae (Figs. 3C-F). In the experiments below, we used *Lmo4^{lacZ/lacZ}* mice and hereafter refer to these mutants as *Lmo4*-nulls.

Defect of Canal Pouch Outgrowth in the Lmo4-null Inner Ear

During the vestibular morphogenesis, the three semicircular canals arise from epithelial outpouches emerging from the otocyst in a sequential fashion: first, a common vertical outpouch develops into the anterior and posterior canals at around E11.5; next, a horizontal outpouch grows into the lateral canal at E12. In the process of canal formation, the opposing walls of these outpouches approach each other to form fusion plates. Then, fusion plates fuse and resorb to form tube-shaped canals (Bissonnette and Fekete, 1996). To determine whether the absence of canals in *Lmo4*-null mice was due to a failure in the canal outpouch formation, an absence of fusion plate formation, or a failure for fusion plates to resorb, we paint-filled the inner ear labyrinth at E11.5 to examine the formation of canal outpouches. While the vertical canal outpouch was readily detected in control inner ear at this stage, this structure was absent in *Lmo4*-null inner ears (Fig. 3B; n=5), indicating that *Lmo4*-nulls are defective in the canal pouch outgrowth.

To investigate whether the absence of canal outpouches in *Lmo4*-null mice is caused by the change in cell proliferation within the presumptive canal regions in the dorsal otocyst, we pulse-labeled mitotic cells at S-phase with 5-bromo, 2'-deoxy-uridine (BrdU) and compared the distribution and number of BrdU$^+$ proliferating cells. At E11.5, the regions with a high density of BrdU$^+$ cells in the control inner ear were detected at the edges of the developing canal plates (Figs. 4B, C; brackets). However, cell proliferation in the corresponding otic regions in *Lmo4*-nulls was greatly reduced (Figs. 4D-F; n=5). X-Gal stained sections further revealed the differences in the dorsal otocysts of *Lmo4* heterozygous and null embryos. In control embryos, the lateral wall of the dorsal otocyst invaginated medially to meet the medial wall and a small region of the dorsolateral otic epithelium became thinner. As the thinned otic epithelial layer continued invaginating medially, it lost the epithelial morphology and the sharp boundary with the peri-otic mesenchyme, and formed the fusion plate (Figs. 4G; arrowheads). The fusion plate then grew more medially and the epithelial cells intercalated to fuse into a single layer, which eventually disappears and leaves behind an intact semicircular duct (Fig. 4G*)*. Although *Lmo4*-null mice lack the prominent vertical canal outpouch (Fig. 3B)*,* regional thinning of the lateral otic epithelium (Fig. 4I; arrowhead) and the rudiment of epithelial invagination at the posterolateral boundary of the inner ear (Fig. 4J; arrowhead) could be observed. However, the invagination is less thorough and the epithelial cells did not push inward within close proximity of the medial layer. Thus, the reduction in cell proliferation and the defective invagination likely result in the failure to form the canal outpouch and lead to the eventual loss of semicircular canals and ampullae in *Lmo4*-null mice.

We further investigated whether the loss of *Lmo4* resulted in a change in apoptosis of the developing inner ear. We immunolabeled serial cryosections of otocysts with anti-activated caspase-3, a marker for apoptotic cells. From E10.5 to E11.5, the apoptotic cells in control

otocysts were mainly localized in the developing endolymphatic duct and in the ventromedial otocyst (Figs. 5A-D) (Fekete et al., 1997; Merlo et al., 2002; Nishikori et al., 1999; Nishizaki et al., 1998). In the *Lmo4*-null otocyst, the number of apoptotic cells in the developing endolymphatic duct was reduced (Fig. 5G; arrowhead). However, the number of apoptotic cells in the ventromedial region of *Lmo4*-null otocyst was dramatically increased (Figs. 5E, F; arrows). Quantification of the caspase-3^{+} apoptotic cells revealed 3.3- and 8.2-fold increases in apoptotic cells within ventromedial epithelium of *Lmo4*-null otocysts at E10.5 (n=4) and E11.5 (n=5), respectively (Fig. 5I). In the developing endolymphatic duct, there was no discernible change in apoptosis at E10.5 (n=4) but a 10.5-fold reduction in the number of apoptotic cells in *Lmo4*-null otocysts at E11.5 (n=5) (Fig. 5I).

Expression of Otic Patterning Genes in the Lmo4-null Inner Ear

Cell fate and lineage analysis has revealed that semicircular canals develop from the lateral region of the otocyst (Fekete and Wu, 2002). The defect in semicircular canals of *Lmo4*-null inner ears is consistent with its restricted expression in the dorsolateral otocyst. To investigate the potential patterning role of *Lmo4* in the developing otic epithelium and to explore the molecular basis of *Lmo4* function, we asked whether *Lmo4*-null mutation altered the expression of genes with established roles in patterning the otocyst by in situ hybridization of the otocyst at E10.5. Previously, when we compared the expression pattern of *Lmo4*-lacZ in *Lmo4*[lacZ/+] and *Lmo4*[lacZ/lacZ] mice, we found that the compartmentalized expression of *Lmo4*-lacZ was maintained in the lateral otocyst (Figs. 2I, J), suggesting that *Lmo4* could be dispensable in the initial patterning and subdivision of the otocyst into different compartments. Consistent with this notion, no evident change or shift was detected in the expression domain of *Hmx2* (Fig. 6A; n=12) and *Hmx3* (Fig. 6B; n=12) in the dorsolateral otocyst, which marks the future vestibular region within the otocyst and is essential for the development of semicircular canals, saccule, and utricle (Wang et al., 2001; Wang et al., 2004b). Furthermore, there was no change in the expression domains of *Lmx1a* (Fig. 6C; n=6) and *Gbx2* (Fig. 6D; n=3) in the dorsal otocyst (Giraldez, 1998) and in the endolymphatic duct precursor within the dorsomedial otocyst (Lin et al., 2005), respectively. In the ventral otocyst, the overlapping expression of *Sox2*, *Otx1*, and *Otx2* demarcate the ventral-most region of the otocyst, a region marking the future cochlear duct (Kiernan et al., 2005; Lillevali et al., 2004; Morsli et al., 1999). Additionally, *Otx1* is expressed more dorsally along the lateral wall of the otocyst, a region contributing to the lateral semicircular canals and ampulla (Morsli et al., 1999). No overt change in the regional expression of these markers was observed in *Lmo4*-null otocysts compared with control otocysts (Figs. 6E-G; n=3). No significant change in the compartmentalized expression of *Lfng* (Fig. 6H; n=6), *Foxg1* (Fig. 6I; n=3), and *Eya2* (Fig. 6J; n=3) in otocysts was observed, either. Thus, *Lmo4* is not essential for the initial compartmentalization of the otocyst.

In the otocyst, the expression of homeobox gene *Dlx5* is confined mostly to the dorsal region, including the developing endolymphatic duct and three discrete nonsensory epithelial patches which are located next to the *Bmp4*-positive sensory domains (the presumptive three cristae) (Acampora et al., 1999; Depew et al., 1999). Mice null for *Dlx5* lack the semicircular canals and have a shorter or absent endolymphatic duct (Merlo et al., 2002), a phenotype resembling that of *Lmo4*-null mice. In *Lmo4*-null mice, the onset of *Dlx5* expression in the otic placode at E8 to E8.5 was unaffected (data not shown). However, its expression in the dorsolateral region of the early otocyst at E9.5 began to be down-regulated (Fig. S3A; arrows; n=3). By E10.5, *Dlx5* expression in the dorsolateral otocyst (brackets) was significantly down regulated while its expression in the dorsomedial otocyst (arrowheads), a region later giving rise to the endolymphtic duct, was unaffected (Fig. 7A; n=12). At E11.5, compared to *Dlx5* expression in three segregated patches in the dorsolateral otocyst of controls, *Dlx5* expression was detected as a single dorsolateral domain in *Lmo4*-null otocyst (Fig. 7F; arrows; n=6).

Gata3, a GATA family member of the zinc finger domain transcription factors, is normally expressed in the dorsolateral and ventromedial ends of otocyst at E10.5 (Fig. 7B) (Lawoko-Kerali et al., 2002). Targeted deletion of *Gata3* leads to an early blockage of inner ear morphogenesis that affects both the vestibular and cochlear development (Karis et al., 2001). In *Lmo4*-null mice, *Gata3* expression was decreased initially at E9.5 (Fig. S3B). At E10.5, it was abolished in the dorsolateral otocyst and was down-regulated in the ventromedial otocyst (Fig. 7B; n=8). Later at E11.5, compared with *Gata3* expression in the developing cristae primordia epithelium of the control ear, no *Gata3* expression was seen in the dorsal part of the *Lmo4*-null ear (Fig. 7G; n=6). Thus, although *Lmo4* is not required for the initial compartmentalization of the otocyst, targeted disruption of *Lmo4* specifically affects the expression of genes expressed in the dorsolateral and ventromedial otocyst.

Lmo4 is required for the expression of genes in the developing cristae

Previously, we have shown that *Lmo4* expression overlaps that of *Bmp4* in the dorsolateral otocyst (Deng et al., 2006). The absence of the cristae primordia in *Lmo4*-nulls prompted us to investigate whether the expression of *Bmp4* and *Fgf10*, which demarcates these three presumptive cristae (Morsli et al., 1998; Pauley et al., 2003), was altered in *Lmo4*-nulls. *Bmp4*, a member of the transforming growth factor-β (TGFß) gene family, is expressed in two distinct areas in the otocyst at E9.5 to E10.5, a posterior domain being the precursor of the posterior crista and an anterior domain being the precursor of the anterior and lateral cristae (Figs. 7C, S3C). In *Lmo4*-nulls, *Bmp4* expression became down-regulated initially at E9.5 (Fig. S3C; n=6). At E10.5, its expression in *Lmo4*-nulls was greatly reduced in the anterior area (arrows) and was abolished in the posterior domain (arrowheads) (Fig. 7C; n=12). Likewise, the expression of *Fgf10*, a member of the *Fgf* superfamily, and *Isl1*, a LIM-homeobox gene, overlapped with *Bmp4* expression in the anterior and posterior pole of the otocyst and was also observed in the developing cochleovestibular ganglion (CVG) (Figs. 7D, E). In *Lmo4*-nulls, their expression was eliminated in the posterior domain and was significantly down regulated in the anterior area (Figs. 7D, E; n=5). At E11.5, in contrast to *Bmp4* expression in three presumptive cristae in the controls, residual *Bmp4* expression was only detected in the dorsoposterior part of *Lmo4*-null otocysts (Fig. 7H; n=6). Moreover, the expression of *Fgf10* and *Isl1*, as well as *Msx1* and *Gata3*, in the presumptive cristae was completely eradicated in *Lmo4*-null inner ear (Figs. 7I-K; n=5). These results demonstrated that *Lmo4* is required for the proper expression of genes during crista formation.

Discussion

In this study, we have demonstrated that the nuclear LMO4 plays a crucial role in the development of the inner ear vestibular organ. We show that *Lmo4* is one of the first genes to be expressed in the otic placode. Later, its expression is seen in the lateral wall of the newly formed otocyst. As the inner ear development proceeds, its expression becomes localized to the dorsolateral otocyst and later to the semicircular canals. Targeted disruption of *Lmo4* in mice does not affect the formation of otic vesicle, indicating that *Lmo4* is dispensable in the induction of otic placode or the initial morphogenesis of the otocyst. In addition, loss of *Lmo4* does not affect early otic compartmentization. However, loss of *Lmo4* results in the complete ablation of three semicircular canals, anterior and posterior cristae. The defects observed in semicircular canals and cristae of *Lmo4*-null mice are consistent with the restricted expression of *Lmo4* in the lateral region of the otocyst. Our results demonstrate that during the vestibular morphogenesis, *Lmo4* likely functions downstream of the otic patterning genes to manifest vestibular structures by stimulating cell proliferation and maintaining the expression of genes in the dorsolateral otocyst.

The proliferation of canal epithelial cells requires LMO4 function

LMO family proteins contain two tandem zinc-finger LIM domains that mediate protein-protein interactions (Bach, 2000). Forced expression of LMO2 in erythroids or LMO4 in mammary epithelial cells and their co-factor LIM-domain-binding protein 1 (LDB1) block the differentiation of erythroids and mammary epithelial cells (Visvader et al., 1997; Visvader et al., 2001). Strong expression of *Lmo4* is frequently observed in proliferating cells, such as the crypt cells of the small intestine and the basal cells of the skin and tongue (Sum et al., 2005a). *Lmo4* is overexpressed in breast cancer and oral cavity carcinomas and the overexpression of *Lmo4* in mice leads to hyperplasia and tumor formation (Mizunuma et al., 2003; Sum et al., 2005a; Sum et al., 2005b; Visvader et al., 2001; Wang et al., 2004a). These findings suggest that LMO proteins are important regulators of epithelial proliferation.

In the otocyst, *Lmo4* is highly expressed in the newly formed epithelial semicircular ducts as the anterior and posterior semicircular canals begin to develop. In *Lmo4*-nulls, the cell proliferation within the dorsolateral otocyst is greatly impaired just before the semicircular epithelium begins to develop, resulting in the failure of canal outpouch formation and ultimately in the dysmorphogenesis of the semicircular systems. Our results indicate that one role of LMO4 is to maintain the proliferation of otic epithelial cells during early inner ear morphogenesis.

Functional relationship Lmo4 and other otic patterning genes

The early onset of *Lmo4* expression in the presumptive vestibule and its subsequent localization in the epithelium of the developing semicircular canals coincides with the initial patterning of the otocyst by otic patterning transcription factors to compartmentalize the otocyst (Torres and Giraldez, 1998). Surprisingly, our expression studies have shown that in the absence of *Lmo4*, the expression domain of *Lmo4*-lacZ in the otocyst is unchanged at early stages. Additionally, we have found no difference in the expression the otic patterning genes in wild type and *Lmo4*-null otocysts (Fig. 6). Therefore, *Lmo4* is unlikely involved in the initial patterning of the otocyst nor does it function upstream of the above otic patterning genes. However, loss of *Lmo4* results in the down-regulation of *Dlx5* specifically in the dorsolateral otocyst from E9.5 while the onset of *Dlx5* expression in the otic placode and the early otocyst at E8.5 is not affected (Figs. 7 and S3). Interestingly, the vestibular defect in *Lmo4*-null inner ear closely resembles those observed in *Dxl5*-null mice that lack the semicircular canals (Acampora et al., 1999; Merlo et al., 2002). Similar to *Lmo4*-null mutation, loss of *Dlx5* results in the absence of a distinct area of cell proliferation in the canal-forming region of the otocyst. Our results demonstrate that *Lmo4* is required to maintain *Dlx5* expression in the dorsolateral otocyst. Thus, the loss of semicircular canal defects in the *Lmo4*-null inner ear could result from the change in the expression of genes such as *Dlx5* in the dorsolateral otocyst and *Lmo4* and *Dlx5* are two components of the transcription factor cascade that governs the semicircular system development.

It remains to be understood how LMO4 regulates the expression of genes within the dorsolateral otocyst. LMO proteins do not bind DNA but are thought to function as molecular adaptors to mediate the protein-protein interaction with other transcription factors. LMO proteins can interact with nuclear LIM-domain-binding (LDB) proteins, as well as LIM-homeodomain proteins via their LIM-domains (Agulnick et al., 1996; Breen et al., 1998; Jurata and Gill, 1997; Jurata et al., 1996). Additionally, LMO2 can form protein complexes with hematopoietic transcription factors SCL/TAL1 and GATA1 (Wadman et al., 1997). Similarly, LMO4 has been found in complexes containing DEAF-1 (Sugihara et al., 1998), BRCA1 and CtIP (Sum et al., 2002), or HEN1 (Manetopoulos et al., 2003). Currently, the transcription factors interacting with LMO4 in the otocyst are yet to be identified. Interestingly, GATA3 is expressed in the dorsolateral and ventromedial domains of the otocycst and is required for

the morphogenesis of the inner ear. The inner ear of *Gata3*-null mice contains a single extension of the endolymphatic duct but lacks semicircular canals and saccular and utricular recesses (Karis et al., 2001). ISL1 is expressed in inner ear neuronal and sensory lineages from very early stages, suggesting its likely role in the development of inner ear neurons and sensory epithelia cells (Li et al., 2004; Radde-Gallwitz et al., 2004). Based on the ability of LMO-class proteins to interact with GATA-family factors (Wadman et al., 1997) and to compete against LIM-homeodomain factors in binding to LDB proteins (Agulnick et al., 1996; Breen et al., 1998; Wadman et al., 1997), it is conceivable that LMO4 could regulate the transcriptional activities of GATA3 and ISL1. The combined expression and action of these factors could provide the combinatory code of transcription factors to define the vestibular identity of the dorsolateral otocyst.

Requirement for Lmo4 in the vestibular development

It has been hypothesized that the interaction between the otic epithelial cells and the surrounding peri-otic mesenchyme plays an important role in the vestibular morphogenesis (Salminen et al., 2000). *Lmo4* is expressed in the otocyst as well as in the peri-otic mesenchyme during the period of vestibular morphogenesis (Fig. 2). Thus, the vestibular defect observed in *Lmo4*-null mice could result from the lack of LMO4 in the otic epithelium or peri-otic mesenchyme or both. To distinguish these possibilities, we have generated the *Lmo4* conditional knockout allele and have used *Foxg1-Cre* to delete *Lmo4* specifically in the otic epithelium while the expression of *Lmo4* in the peri-otic mesenchyme is not affected (Fig. 1D). The conditional removal of *Lmo4* in the otic epithelium alone results in the vestibular defect identical to that observed *Lmo4$^{lacZ/lacZ}$* mice, indicating that the expression of *Lmo4* in the otic epithelium is essential for normal vestibular development. However, since the *Lmo4*-null mutation results in the failure in the initial pouch formation (Fig. 3B), we are unable to determine whether the persistent *Lmo4* expression in the otic epithelium and the peri-otic mesenchyme is required for the fusion plate formation and other later events. Future experiments of the peri-otic mesenchyme-specific deletion of *Lmo4* and removal of *Lmo4* after the formation of canal outpouches using the peri-otic mesenchyme-specific Cre and otic-specific, inducible Cre mouse lines will help to address these questions. At the cellular level, the defects in the formation of semicircular canals and ampullae in *Lmo4*-null mice likely result from the defective cell proliferation as loss of *Lmo4* causes a reduction in cell proliferation in the otic regions corresponding to the developing canal pouch (Fig. 6).

By examining the programmed cell death in the developing inner ear, we have also demonstrated an increase in apoptosis of the ventromedial otocyst and a reduced apoptosis level in the developing endolymphatic duct, where *Lmo4* expression is not detected. Since the expression of *Gata3* in the ventromedial domain is down-regulated in *Lmo4*-null otocysts (Fig. 7B), loss of *Lmo4* likely functions in a non-cell-autonomous manner to regulate genes, such as *Gata3* and others, in the ventromedial otocyst. Similarly, the shorter cochlea in *Lmo4*-null inner ear could be an indirect consequence of *Lmo4*-null mutation that causes the elevated cell death in the corresponding ventromedial compartment that could lead a reduction of progenitor cells to drive cochleogenesis. The functional importance of the altered apoptosis pattern in *Lmo4*-null mice is unknown. However, mice deficient for *Dlx5*, *Hmx2*, and *Hmx3* exhibit a very similar malformation of the semicircular canals and a similar increase in cell death in the ventromedial otocyst (Merlo et al., 2002;Wang et al., 2001;Wang et al., 2004b;Wang and Lufkin, 2005;Wang et al., 1998). Moreover, the broader endolymphatic duct observed in *Lmo4*-null mice could be the consequence of the reduced level of apoptosis in the corresponding otic region.

Requirement for Lmo4 in crista formation

Lmo4 is expressed in both the non-sensory and sensory domains of the vestibular epithelium during semicircular duct outgrowth (Chang et al., 2008; Deng et al., 2006). In addition to being essential in the growth of semicircular duct epithelium, *Lmo4* plays an important role in the formation of the semicircular sensory cristae. In the absence of *Lmo4*, anterior and posterior cristae primordia fail to develop (Fig. 3A). Our expression study further reveals that *Lmo4* is required for the proper expression of crista-associated genes, specifically, for the maintenance of *Bmp4*, *Fgf10*, and *Gata3* expression and the activation of *Msx1* and *Isl1* expression in the dorsolateral otocyst (Figs. 7 and S3). Thus, *Lmo4* likely regulates the crista formation by controlling the expression of these crista-associated genes. Previously, *Bmp4* has been reported to play a key role in the formation of all three semicircular canals and their sensory cristae (Chang et al., 2008; Cole et al., 2000; Merlo et al., 2002; Morsli et al., 1998; Oh et al., 1996). The inner ear-specific knockout of *Bmp4* in mice and down-regulation of *Bmp4* signaling pathway in chicken inner ears results in the loss or down-regulation of crista-associated genes including *Lmo4*, suggesting that *Bmp4* regulate *Lmo4* expression during sensory crista development (Chang et al., 2008). Interestingly, we show here that *Bmp4* expression is significantly reduced in *Lmo4*-null embryos. Thus, our results reveal a novel relationship between *Lmo4* and *Bmp4* that *Lmo4* and *Bmp4* mutually regulate each others' expression and jointly control the expression of crista-associated genes during crista formation.

Moreover, FGF signaling pathway plays an important role in patterning the otic vesicle including otic induction, morphogenesis, hair cell and pillar cell development (Alvarez et al., 2003; Jacques et al., 2007; Mansour et al., 1993; Mueller et al., 2002; Pauley et al., 2003; Shim et al., 2005; Wright and Mansour, 2003a; Wright and Mansour, 2003b). *Fgf10* is expressed in all three cristae sensory epithelia and *Fgf10*-null mutants lack the semicircular canals and the posterior crista (Pauley et al., 2003). In the *Lmo4*-null otocyst, *Fgf10* expression in the cristae is lost. Previously, it has been reported that *Fgf10* expression is abolished in *Gata3*-null otic epithelium (Lillevali et al., 2006). Since LMO2 and GATA1 are shown to interact directly and form a transcriptional complex with other transcription factors in erythroid cells (Wadman et al., 1997), it is plausible that LMO4 could regulate *Fgf10* expression by interacting with GATA3 or other factors. Taken together, our results demonstrate the essential role of *Lmo4* in the development of cristae. Future studies on the mechanism of LMO4 function will shed light on the regulation of the crista formation, a complicated process that is controlled by many specific factors.

Supplementary Material

Refer to Web version on PubMed Central for supplementary material.

Acknowledgments

References

Acampora D, Merlo GR, Paleari L, Zerega B, Postiglione MP, Mantero S, Bober E, Barbieri O, Simeone A, Levi G. Craniofacial, vestibular and bone defects in mice lacking the Distalless-related gene Dlx5. Development 1999;126:3795–809. [PubMed: 10433909]

Adamska M, Herbrand H, Adamski M, Kruger M, Braun T, Bober E. FGFs control the patterning of the inner ear but are not able to induce the full ear program. Mech Dev 2001;109:303–13. [PubMed: 11731242]

Agulnick AD, Taira M, Breen JJ, Tanaka T, Dawid IB, Westphal H. Interactions of the LIM-domain-binding factor Ldb1 with LIM homeodomain proteins. Nature 1996;384:270–2. [PubMed: 8918878]

Alvarez Y, Alonso MT, Vendrell V, Zelarayan LC, Chamero P, Theil T, Bosl MR, Kato S, Maconochie M, Riethmacher D, Schimmang T. Requirements for FGF3 and FGF10 during inner ear formation. Development 2003;130:6329–38. [PubMed: 14623822]

Auerbach W, Dunmore JH, Fairchild-Huntress V, Fang Q, Auerbach AB, Huszar D, Joyner AL. Establishment and chimera analysis of 129/SvEv- and C57BL/6-derived mouse embryonic stem cell lines. Biotechniques 2000;29:1024–8. 1030, 1032. [PubMed: 11084865]

Bach I. The LIM domain: regulation by association. Mech Dev 2000;91:5–17. [PubMed: 10704826]

Baker CV, Bronner-Fraser M. Vertebrate cranial placodes I. Embryonic induction. Dev Biol 2001;232:1–61. [PubMed: 11254347]

Bell D, Streit A, Gorospe I, Varela-Nieto I, Alsina B, Giraldez F. Spatial and temporal segregation of auditory and vestibular neurons in the otic placode. Dev Biol 2008;322:109–20. [PubMed: 18674529]

Bissonnette JP, Fekete DM. Standard atlas of the gross anatomy of the developing inner ear of the chicken. J Comp Neurol 1996;368:620–30. [PubMed: 8744448]

Bober E, Rinkwitz S, Herbrand H. Molecular basis of otic commitment and morphogenesis: a role for homeodomain-containing transcription factors and signaling molecules. Curr Top Dev Biol 2003;57:151–75. [PubMed: 14674480]

Bok J, Dolson DK, Hill P, Ruther U, Epstein DJ, Wu DK. Opposing gradients of Gli repressor and activators mediate Shh signaling along the dorsoventral axis of the inner ear. Development 2007;134:1713–22. [PubMed: 17395647]

Breen JJ, Agulnick AD, Westphal H, Dawid IB. Interactions between LIM domains and the LIM domain-binding protein Ldb1. J Biol Chem 1998;273:4712–7. [PubMed: 9468533]

Burton Q, Cole LK, Mulheisen M, Chang W, Wu DK. The role of Pax2 in mouse inner ear development. Dev Biol 2004;272:161–75. [PubMed: 15242798]

Chang W, Brigande JV, Fekete DM, Wu DK. The development of semicircular canals in the inner ear: role of FGFs in sensory cristae. Development 2004;131:4201–11. [PubMed: 15280215]

Chang W, Lin Z, Kulessa H, Hebert J, Hogan BL, Wu DK. Bmp4 is essential for the formation of the vestibular apparatus that detects angular head movements. PLoS Genet 2008;4:e1000050. [PubMed: 18404215]

Chang W, Nunes FD, De Jesus-Escobar JM, Harland R, Wu DK. Ectopic noggin blocks sensory and nonsensory organ morphogenesis in the chicken inner ear. Dev Biol 1999;216:369–81. [PubMed: 10588886]

Cole LK, Le Roux I, Nunes F, Laufer E, Lewis J, Wu DK. Sensory organ generation in the chicken inner ear: contributions of bone morphogenetic protein 4, serrate1, and lunatic fringe. J Comp Neurol 2000;424:509–20. [PubMed: 10906716]

Deng M, Pan L, Xie X, Gan L. Differential expression of LIM domain-only (LMO) genes in the developing mouse inner ear. Gene Expr Patterns 2006;6:857–63. [PubMed: 16597514]

Depew MJ, Liu JK, Long JE, Presley R, Meneses JJ, Pedersen RA, Rubenstein JL. Dlx5 regulates regional development of the branchial arches and sensory capsules. Development 1999;126:3831–46. [PubMed: 10433912]

Fekete DM. Cell fate specification in the inner ear. Curr Opin Neurobiol 1996;6:533–41. [PubMed: 8794105]

Fekete DM, Homburger SA, Waring MT, Riedl AE, Garcia LF. Involvement of programmed cell death in morphogenesis of the vertebrate inner ear. Development 1997;124:2451–61. [PubMed: 9199371]

Fekete DM, Wu DK. Revisiting cell fate specification in the inner ear. Curr Opin Neurobiol 2002;12:35–42. [PubMed: 11861162]

Fritzsch B, Beisel KW, Jones K, Farinas I, Maklad A, Lee J, Reichardt LF. Development and evolution of inner ear sensory epithelia and their innervation. J Neurobiol 2002;53:143–56. [PubMed: 12382272]

Gan L, Wang SW, Huang Z, Klein WH. POU domain factor Brn-3b is essential for retinal ganglion cell differentiation and survival but not for initial cell fate specification. Dev Biol 1999;210:469–80. [PubMed: 10357904]

Gerlach LM, Hutson MR, Germiller JA, Nguyen-Luu D, Victor JC, Barald KF. Addition of the BMP4 antagonist, noggin, disrupts avian inner ear development. Development 2000;127:45–54. [PubMed: 10654599]

Giraldez F. Regionalized organizing activity of the neural tube revealed by the regulation of lmx1 in the otic vesicle. Dev Biol 1998;203:189–200. [PubMed: 9806783]

Hahm K, Sum EY, Fujiwara Y, Lindeman GJ, Visvader JE, Orkin SH. Defective neural tube closure and anteroposterior patterning in mice lacking the LIM protein LMO4 or its interacting partner Deaf-1. Mol Cell Biol 2004;24:2074–82. [PubMed: 14966286]

Hatch EP, Noyes CA, Wang X, Wright TJ, Mansour SL. Fgf3 is required for dorsal patterning and morphogenesis of the inner ear epithelium. Development 2007;134:3615–25. [PubMed: 17855431]

Hebert JM, McConnell SK. Targeting of cre to the Foxg1 (BF-1) locus mediates loxP recombination in the telencephalon and other developing head structures. Dev Biol 2000;222:296–306. [PubMed: 10837119]

Jacques BE, Montcouquiol ME, Layman EM, Lewandoski M, Kelley MW. Fgf8 induces pillar cell fate and regulates cellular patterning in the mammalian cochlea. Development 2007;134:3021–9. [PubMed: 17634195]

Jurata LW, Gill GN. Functional analysis of the nuclear LIM domain interactor NLI. Mol Cell Biol 1997;17:5688–98. [PubMed: 9315627]

Jurata LW, Kenny DA, Gill GN. Nuclear LIM interactor, a rhombotin and LIM homeodomain interacting protein, is expressed early in neuronal development. Proc Natl Acad Sci U S A 1996;93:11693–8. [PubMed: 8876198]

Karis A, Pata I, van Doorninck JH, Grosveld F, de Zeeuw CI, de Caprona D, Fritzsch B. Transcription factor GATA-3 alters pathway selection of olivocochlear neurons and affects morphogenesis of the ear. J Comp Neurol 2001;429:615–30. [PubMed: 11135239]

Kiernan AE, Pelling AL, Leung KK, Tang AS, Bell DM, Tease C, Lovell-Badge R, Steel KP, Cheah KS. Sox2 is required for sensory organ development in the mammalian inner ear. Nature 2005;434:1031–5. [PubMed: 15846349]

Ladher RK, Wright TJ, Moon AM, Mansour SL, Schoenwolf GC. FGF8 initiates inner ear induction in chick and mouse. Genes Dev 2005;19:603–13. [PubMed: 15741321]

Lawoko-Kerali G, Rivolta MN, Holley M. Expression of the transcription factors GATA3 and Pax2 during development of the mammalian inner ear. J Comp Neurol 2002;442:378–91. [PubMed: 11793341]

Lee SK, Jurata LW, Nowak R, Lettieri K, Kenny DA, Pfaff SL, Gill GN. The LIM domain-only protein LMO4 is required for neural tube closure. Mol Cell Neurosci 2005;28:205–14. [PubMed: 15691703]

Li H, Liu H, Sage C, Huang M, Chen ZY, Heller S. Islet-1 expression in the developing chicken inner ear. J Comp Neurol 2004;477:1–10. [PubMed: 15281076]

Li JY, Joyner AL. Otx2 and Gbx2 are required for refinement and not induction of mid-hindbrain gene expression. Development 2001;128:4979–91. [PubMed: 11748135]

Lillevali K, Haugas M, Matilainen T, Pussinen C, Karis A, Salminen M. Gata3 is required for early morphogenesis and Fgf10 expression during otic development. Mech Dev 2006;123:415–29. [PubMed: 16806848]

Lillevali K, Matilainen T, Karis A, Salminen M. Partially overlapping expression of Gata2 and Gata3 during inner ear development. Dev Dyn 2004;231:775–81. [PubMed: 15499560]

Lin Z, Cantos R, Patente M, Wu DK. Gbx2 is required for the morphogenesis of the mouse inner ear: a downstream candidate of hindbrain signaling. Development 2005;132:2309–18. [PubMed: 15829521]

Lumsden A, Krumlauf R. Patterning the vertebrate neuraxis. Science 1996;274:1109–15. [PubMed: 8895453]

Manetopoulos C, Hansson A, Karlsson J, Jonsson JI, Axelson H. The LIM-only protein LMO4 modulates the transcriptional activity of HEN1. Biochem Biophys Res Commun 2003;307:891–9. [PubMed: 12878195]

Mansour SL, Goddard JM, Capecchi MR. Mice homozygous for a targeted disruption of the proto-oncogene int-2 have developmental defects in the tail and inner ear. Development 1993;117:13–28. [PubMed: 8223243]

Merlo GR, Paleari L, Mantero S, Zerega B, Adamska M, Rinkwitz S, Bober E, Levi G. The Dlx5 homeobox gene is essential for vestibular morphogenesis in the mouse embryo through a BMP4-mediated pathway. Dev Biol 2002;248:157–69. [PubMed: 12142028]

Mishina Y, Suzuki A, Ueno N, Behringer RR. Bmpr encodes a type I bone morphogenetic protein receptor that is essential for gastrulation during mouse embryogenesis. Genes Dev 1995;9:3027–37. [PubMed: 8543149]

Mizunuma H, Miyazawa J, Sanada K, Imai K. The LIM-only protein, LMO4, and the LIM domain-binding protein, LDB1, expression in squamous cell carcinomas of the oral cavity. Br J Cancer 2003;88:1543–8. [PubMed: 12771919]

Morsli H, Choo D, Ryan A, Johnson R, Wu DK. Development of the mouse inner ear and origin of its sensory organs. J Neurosci 1998;18:3327–35. [PubMed: 9547240]

Morsli H, Tuorto F, Choo D, Postiglione MP, Simeone A, Wu DK. Otx1 and Otx2 activities are required for the normal development of the mouse inner ear. Development 1999;126:2335–43. [PubMed: 10225993]

Mueller KL, Jacques BE, Kelley MW. Fibroblast growth factor signaling regulates pillar cell development in the organ of corti. J Neurosci 2002;22:9368–77. [PubMed: 12417662]

Nishikori T, Hatta T, Kawauchi H, Otani H. Apoptosis during inner ear development in human and mouse embryos: an analysis by computer-assisted three-dimensional reconstruction. Anat Embryol (Berl) 1999;200:19–26. [PubMed: 10395002]

Nishizaki K, Anniko M, Orita Y, Karita K, Masuda Y, Yoshino T. Programmed cell death in the developing epithelium of the mouse inner ear. Acta Otolaryngol 1998;118:96–100. [PubMed: 9504171]

O'Leary DD, Nakagawa Y. Patterning centers, regulatory genes and extrinsic mechanisms controlling arealization of the neocortex. Curr Opin Neurobiol 2002;12:14–25. [PubMed: 11861160]

Oh SH, Johnson R, Wu DK. Differential expression of bone morphogenetic proteins in the developing vestibular and auditory sensory organs. J Neurosci 1996;16:6463–75. [PubMed: 8815925]

Ohyama T, Mohamed OA, Taketo MM, Dufort D, Groves AK. Wnt signals mediate a fate decision between otic placode and epidermis. Development 2006;133:865–75. [PubMed: 16452098]

Pauley S, Wright TJ, Pirvola U, Ornitz D, Beisel K, Fritzsch B. Expression and function of FGF10 in mammalian inner ear development. Dev Dyn 2003;227:203–15. [PubMed: 12761848]

Radde-Gallwitz K, Pan L, Gan L, Lin X, Segil N, Chen P. Expression of Islet1 marks the sensory and neuronal lineages in the mammalian inner ear. J Comp Neurol 2004;477:412–21. [PubMed: 15329890]

Riccomagno MM, Martinu L, Mulheisen M, Wu DK, Epstein DJ. Specification of the mammalian cochlea is dependent on Sonic hedgehog. Genes Dev 2002;16:2365–78. [PubMed: 12231626]

Riccomagno MM, Takada S, Epstein DJ. Wnt-dependent regulation of inner ear morphogenesis is balanced by the opposing and supporting roles of Shh. Genes Dev 2005;19:1612–23. [PubMed: 15961523]

Salminen M, Meyer BI, Bober E, Gruss P. Netrin 1 is required for semicircular canal formation in the mouse inner ear. Development 2000;127:13–22. [PubMed: 10654596]

Shim K, Minowada G, Coling DE, Martin GR. Sprouty2, a mouse deafness gene, regulates cell fate decisions in the auditory sensory epithelium by antagonizing FGF signaling. Dev Cell 2005;8:553–64. [PubMed: 15809037]

Sugihara TM, Bach I, Kioussi C, Rosenfeld MG, Andersen B. Mouse deformed epidermal autoregulatory factor 1 recruits a LIM domain factor, LMO-4, and CLIM coregulators. Proc Natl Acad Sci U S A 1998;95:15418–23. [PubMed: 9860983]

Sum EY, O'Reilly LA, Jonas N, Lindeman GJ, Visvader JE. The LIM domain protein Lmo4 is highly expressed in proliferating mouse epithelial tissues. J Histochem Cytochem 2005a;53:475–86. [PubMed: 15805422]

Sum EY, Peng B, Yu X, Chen J, Byrne J, Lindeman GJ, Visvader JE. The LIM domain protein LMO4 interacts with the cofactor CtIP and the tumor suppressor BRCA1 and inhibits BRCA1 activity. J Biol Chem 2002;277:7849–56. [PubMed: 11751867]

Sum EY, Segara D, Duscio B, Bath ML, Field AS, Sutherland RL, Lindeman GJ, Visvader JE. Overexpression of LMO4 induces mammary hyperplasia, promotes cell invasion, and is a predictor of poor outcome in breast cancer. Proc Natl Acad Sci U S A 2005b;102:7659–64. [PubMed: 15897450]

Torres M, Giraldez F. The development of the vertebrate inner ear. Mech Dev 1998;71:5–21. [PubMed: 9507049]

Torres M, Gomez-Pardo E, Gruss P. Pax2 contributes to inner ear patterning and optic nerve trajectory. Development 1996;122:3381–91. [PubMed: 8951055]

Tse E, Smith AJ, Hunt S, Lavenir I, Forster A, Warren AJ, Grutz G, Foroni L, Carlton MB, Colledge WH, Boehm T, Rabbitts TH. Null mutation of the Lmo4 gene or a combined null mutation of the Lmo1/Lmo3 genes causes perinatal lethality, and Lmo4 controls neural tube development in mice. Mol Cell Biol 2004;24:2063–73. [PubMed: 14966285]

Visvader JE, Mao X, Fujiwara Y, Hahm K, Orkin SH. The LIM-domain binding protein Ldb1 and its partner LMO2 act as negative regulators of erythroid differentiation. Proc Natl Acad Sci U S A 1997;94:13707–12. [PubMed: 9391090]

Visvader JE, Venter D, Hahm K, Santamaria M, Sum EY, O'Reilly L, White D, Williams R, Armes J, Lindeman GJ. The LIM domain gene LMO4 inhibits differentiation of mammary epithelial cells in vitro and is overexpressed in breast cancer. Proc Natl Acad Sci U S A 2001;98:14452–7. [PubMed: 11734645]

Wadman IA, Osada H, Grutz GG, Agulnick AD, Westphal H, Forster A, Rabbitts TH. The LIM-only protein Lmo2 is a bridging molecule assembling an erythroid, DNA-binding complex which includes the TAL1, E47, GATA-1 and Ldb1/NLI proteins. Embo J 1997;16:3145–57. [PubMed: 9214632]

Wang N, Kudryavtseva E, Ch'en IL, McCormick J, Sugihara TM, Ruiz R, Andersen B. Expression of an engrailed-LMO4 fusion protein in mammary epithelial cells inhibits mammary gland development in mice. Oncogene 2004a;23:1507–13. [PubMed: 14676840]

Wang W, Chan EK, Baron S, Van de Water T, Lufkin T. Hmx2 homeobox gene control of murine vestibular morphogenesis. Development 2001;128:5017–29. [PubMed: 11748138]

Wang W, Grimmer JF, Van De Water TR, Lufkin T. Hmx2 and Hmx3 homeobox genes direct development of the murine inner ear and hypothalamus and can be functionally replaced by Drosophila Hmx. Dev Cell 2004b;7:439–53. [PubMed: 15363417]

Wang W, Lufkin T. Hmx homeobox gene function in inner ear and nervous system cell-type specification and development. Exp Cell Res 2005;306:373–9. [PubMed: 15925593]

Wang W, Van De Water T, Lufkin T. Inner ear and maternal reproductive defects in mice lacking the Hmx3 homeobox gene. Development 1998;125:621–34. [PubMed: 9435283]

Wilkinson, DG. Whole Mount in situ Hybridisation of Vertebrate Embryos. IRL Press; Oxford: 1992.

Wright TJ, Mansour SL. Fgf3 and Fgf10 are required for mouse otic placode induction. Development 2003a;130:3379–90. [PubMed: 12810586]

Wright TJ, Mansour SL. FGF signaling in ear development and innervation. Curr Top Dev Biol 2003b; 57:225–59. [PubMed: 14674483]

Zelarayan LC, Vendrell V, Alvarez Y, Dominguez-Frutos E, Theil T, Alonso MT, Maconochie M, Schimmang T. Differential requirements for FGF3, FGF8 and FGF10 during inner ear development. Dev Biol 2007;308:379–91. [PubMed: 17601531]
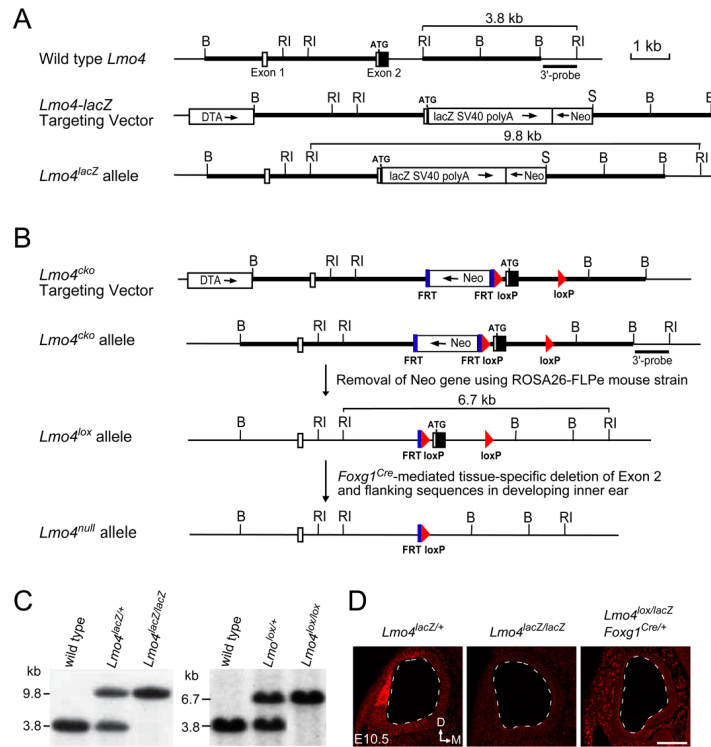
Fig. 1.
Generation of *Lmo4-lacZ* knock-in and *Lmo4* conditional knockout alleles. (A) Generation of *Lmo4-lacZ* (*Lmo4^{lacZ}*) knock-in allele. *Lmo4* genomic structure and restriction enzyme map is shown at the top. Open boxes are the non-coding exon sequences and filled boxes the coding sequences. Thick bars are the sequences used to generate the homologous arms in the targeting vector. The DNA fragment containing reporter *lacZ* and neomycin resistance gene is used to replace the coding region of Exon 2 and a part of Intron 2 in the targeting vector. (B) Generation of *Lmo4* conditional allele. The *Lmo4^{cko}* targeting vector is made by inserting the FRT-flanked neomycin gene and the 5′ loxP sequence in the Intron 1 at 470 bp upsteam of the translation initiation codon. The 3′ loxP sequence is inserted at *EcoRI* site at 1,102 bp downsteam of the translation initiation codon and *EcoRI* site is eliminated. *ROSA26-FLPe* mice are used to remove the neomycin resistance gene in the *Lmo4^{cko}* mice to generate *Lmo4* conditional knockout allele (*Lmo4^{lox}*). Tissue-specific deletion in the inner ear is achieved by crossing *Lmo4^{lox}* mice to *Foxg1-Cre* deleter mice. Abbreviations: Neo, PGK-neomycin resistance gene; DTA, diphtheria toxin gene for negative selection of embryonic stem cells; lacZ, ß-galactosidase reporter gene; FRT, flipase recognition sequence; loxP, Cre recombinase recognition sequence. Restriction enzymes: RI, *EcoRI*; B, *BamHI*; S, *SalI*. (C) Southern genotyping confirmation of *Lmo4^{lacZ}* and *Lmo4^{lox}* mice using 3′ probe and *EcoRI* digestion. (D) Anti-LMO4 immunolabeling of otic cryosections at E10.5 confirms the absence of LMO4 in *Lmo4^{lacZ/lacZ}* mice and the inner ear-specific knockout of *Lmo4* in *Lmo4^{lox/lacZ}*;*Foxg1-Cre* mice. Dashed line outlines the otic vesicles. Scale bar in (D) equals 100 µm.
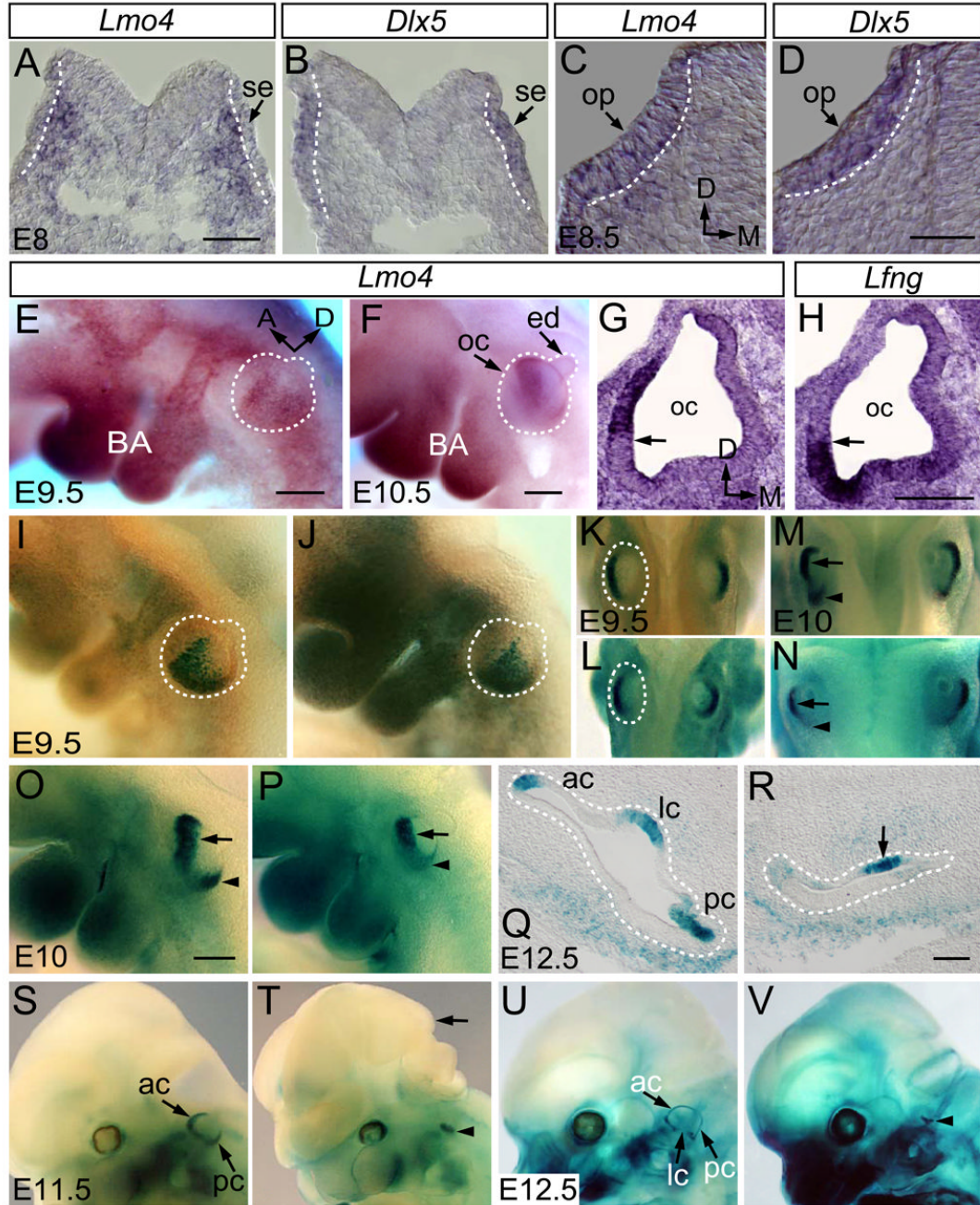
Fig. 2.
Expression of *Lmo4* in developing mouse inner ears and the defective inner ear morphogenesis in *Lmo4*-null mice. (A-D) Expression comparison of *Lmo4* (A, C) and *Dlx5* (B, D) by section in situ hybridization of mouse inner ears at E8 (A, B) and E8.5 (C, D). (E, F) Whole-mount in situ hybridization of *Lmo4* at E9.5 (E) and E10.5 (F) (lateral view). (G, H) Comparison of *Lmo4* (G) and *Lfng* (H) expression by section in situ hybridization of mouse inner ears at E10.5. (I-V) Whole-mount and section X-Gal stained *Lmo4*$^{lacZ/+}$ (I, K, M, O, Q, S and U) and *Lmo4*$^{lacZ/lacZ}$ (J, L, N, P, R, T and V) embryos at E9.5 (I and J, lateral view; K and L, dorsal view), E10 (M and N, dorsal view; O and P, lateral view), E11.5 (S and T, lateral view) and E12.5 (Q and R, section; U and V, lateral view). Abbreviations: se, surface ectoderm; oc,

otocyst; ba, branchial arches; ac, anterior semicircular canal; pc, posterior semicircular canal; lc, lateral semicircular canal; op, otic placode; ed, endolymphatic duct. Dotted white lines mark the otic placodes and otocysts. Orientation of embryos in (E, F, I, J, O, P, and S-V) is indicated in (E). Scale bars: 50 μm in (A) for (A, B); in (D) for (C, D); in (E) for (E, I, J); in (H) for (G, H); in (O) for (O, P); in (R) for (Q, R).
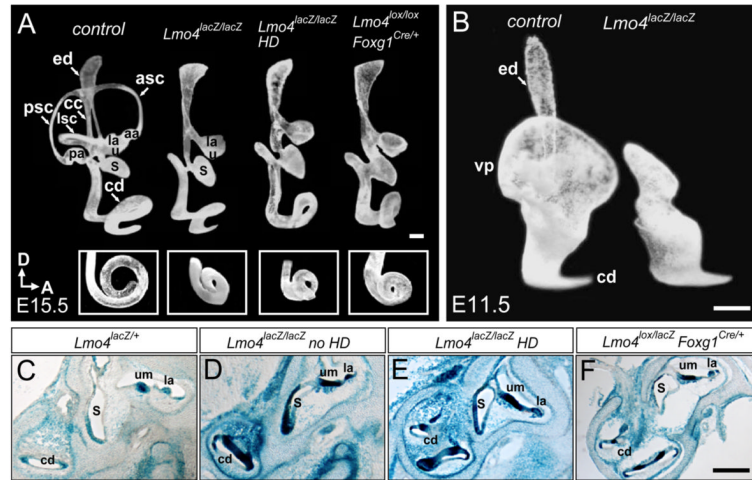
Fig. 3.
The abnormal vestibular morphogenesis in the *Lmo4-null* inner ear. (A) Lateral view of paint-filled wild type (left) and three *Lmo4-null* inner ears at E15.5. Inserts at the bottom are ventral views of the cochleae. All inner ears in *Lmo4-null* mice lack the three semicircular canals, and anterior and posterior ampullae. Compared to one and one-half turns in control cochleae at E15.5, the cochleae of *Lmo4-null* mice are shorter and only have one and one-quarter turns. (B) Lateral view of paint-filled wild type (left) and *Lmo4$^{lacZ/lacZ}$* (right) inner ears at E11.5. *Lmo4$^{lacZ/lacZ}$* inner ear has no visible vertical canal outpouch at this stage. (C-F) Section X-Gal stained *Lmo4$^{lacZ/+}$* (C), *Lmo4$^{lacZ/lacZ}$* (D, no exencephaly; E, exencephaly) and *Lmo4$^{lacZ/lox}$; Foxg1$^{Cre/+}$* (F) inner ears at E18.5. All three kinds of *Lmo4-null* inner ears have macula utriculi and lateral crista. Abbreviations: aa, anterior ampulla; la, lateral ampulla; pa, posterior ampulla; asc, anterior semicircular canal; lsc, lateral semicircular canal; psc, posterior semicircular canal; ed, endolymphatic duct; cc, common crus; vp, vertical canal outpouch; cd, cochlea duct; s, saccule; u, utricle; um, macula utriculi; HD, exencephaly or head defective. Scale bar is 100 μm.
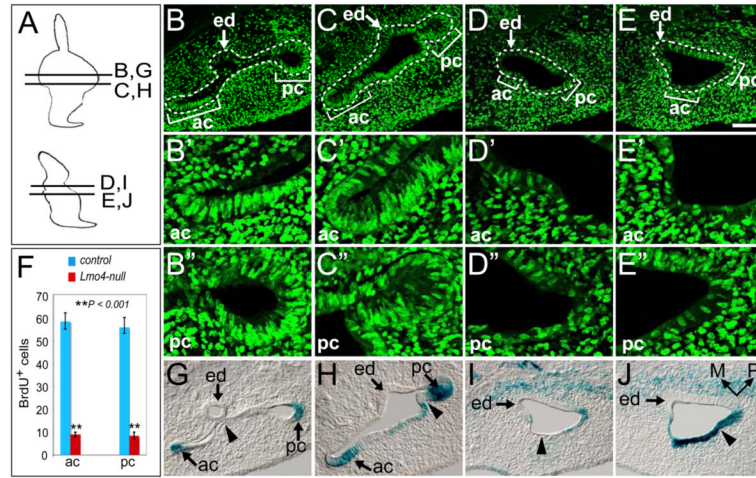
Fig. 4.
Reduced cell proliferation in the dorsal otocyst of *Lmo4-null* mice. (A) Schematic diagrams show the approximate locations of sections shown in (B-E, G-J). (B-E) Immunostaining with anti-BrdU (green) at E11.5 reveals the nuclei of proliferating cells at S-phase in $Lmo4^{lacZ/+}$ (B, C) and $Lmo4^{lacZ/lacZ}$ (D, E) embryos. White dashed lines outline the otic epithelium. Brackets in indicate the approximate areas of anterior (ac) and posterior (pc) semicircular canal epithelium. (B'-E') and (B"-E") are the enlarged images corresponding to the anterior and posterior semicircular canal epithelium regions in (B-E). (F) Quantitative analyses of BrdU-positive cells (proliferating cells) in anterior and posterior semicircular canal areas in control and *Lmo4-null* embryos at E11.5. (G-J) X-Gal stained $Lmo4^{lacZ/+}$ (G, H) and $Lmo4^{lacZ/lacZ}$ (I, J) inner ear sections at E11.5 reveal the morphology and location of the anterior and posterior semicircular canal epithelium regions. (G-J) are the adjacent sections of (B-E). Scale bar equals 100 μm.
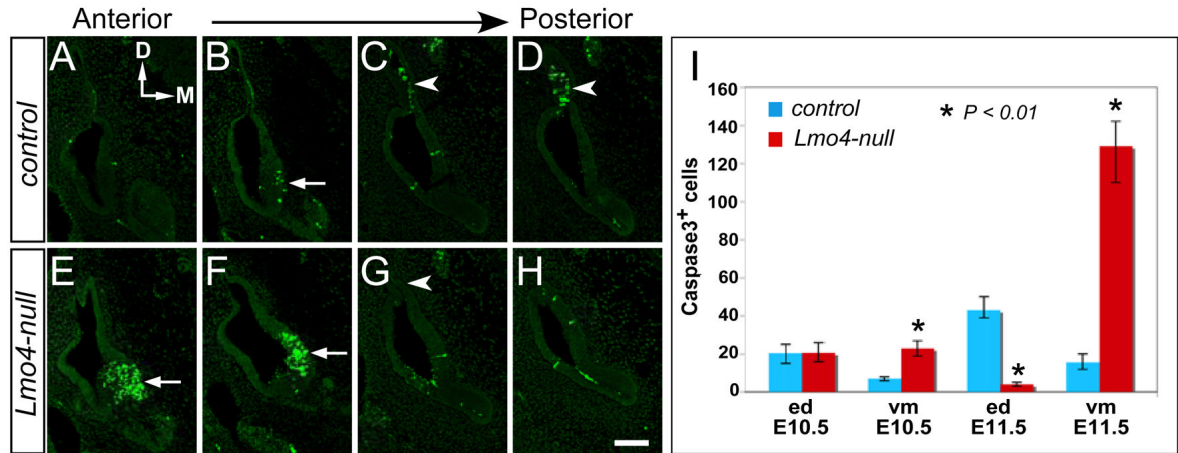
Fig. 5.
Apoptosis in the otocyst of *Lmo4-null* embryos. Anti-activated caspase-3 labeling (green) of adjacent transverse sections from anterior to posterior of otocyst at E11.5. (A-D) In control otocysts, distinctive apoptotic zones are located in the ventromedial otocyst (B; arrow) and along the endolymphatic duct (C and D; arrowheads). (E-H) In *Lmo4-null* otocysts, an increase in apoptotic cells is observed in the anterior ventromedial otocyst (E and F; arrows) whereas the number of apoptotic cells is reduced along the endolymphatic duct. (I) Quantitative analyses of caspase3-postive apoptotic cells in the control and *Lmo4-null* embryos at E10.5 and E11.5. Abbreviations: ed, endolymphatic duct; vm, ventromedial otocyst. Scale bar equals 100 µm.
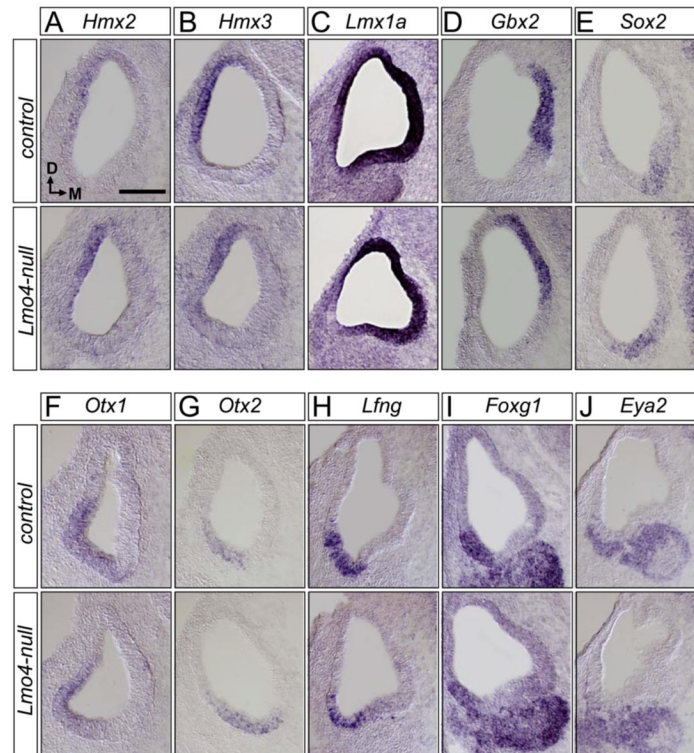
Fig. 6.
Loss of *Lmo4* does not affect the initial patterning of the developing otocyst. Section in situ hybridization of the control and *Lmo4-null* otocysts at E10.5 reveals that the expression patterns of the otic patterning genes, *Hmx2* (A), *Hmx3* (B), *Lmx1a* (C), *Gbx2* (D), *Sox2* (E), *Otx1* (F), *Otx2* (G), *Lfng* (H), *Foxg1* (I), and *Eya2* (J) are not affected in the corresponding region in the *Lmo4-null* otocyst. Orientation in all transverse sections is indicated in (A). Scale bar equals 100 μm.
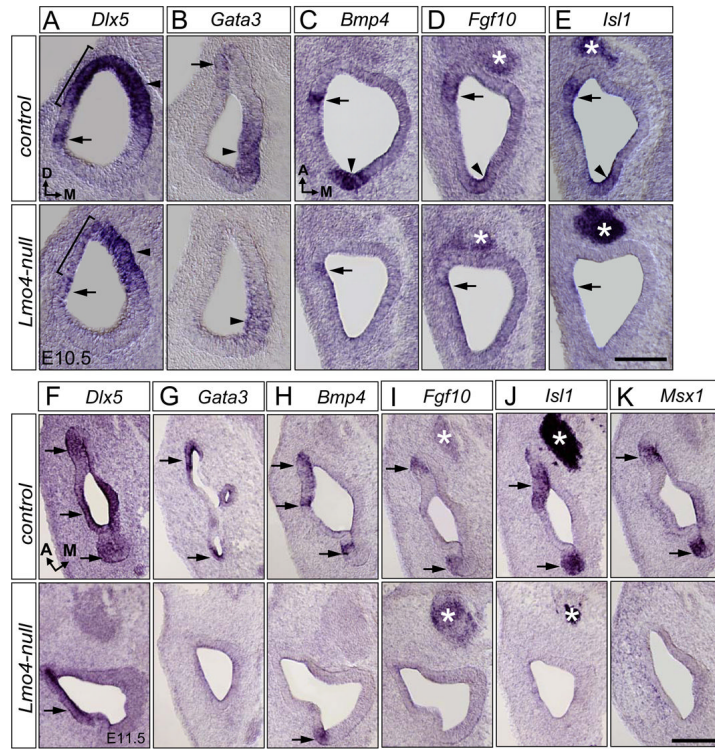
Fig. 7.
Altered expression of the crista-associated genes in *Lmo4*-null mice. Section in situ hybridization of the control (top) and *Lmo4-null* (bottom) otocysts at E10.5 (A-E) and E11.5 (F-K). (A) *Lmo4-null* mutation abolishes the dorsolateral expression domain (bracket) of *Dlx5*. (B) The dorsolateral domain of *Gata3* expression (arrow) is abolished and the ventromedial region (arrowhead) is down-regulated. (C) The posterior domain of *Bmp4* expression is abolished (arrowheads) and its anterior expression domain is significantly reduced (arrow) in the *Lmo4-null* otocyst. (D, E) The expression of *Fgf10* (D) and *Isl1* (E) in the dorsolateral otocyst is overtly down-regulated (arrowheads indicate their posterior expression domain and arrows indicate their anterior expression domain), while their expression in the cochleovestibular ganglion (CVG) is unchanged (asterisks). (F) Expression of *Dlx5* in discrete regions of the lateral portion of the control inner ear is replaced by a homogenous expression in the corresponding region in the *Lmo4-null* embryos (arrows). (G) Loss of *Gata3* expression in the dorsolateral region (arrows) of the *Lmo4*-null inner ear. (H) Significant down-regulation of *Bmp4* expression in the discrete epithelial patches in the dorsolateral part of the *Lmo4*-null inner ear (arrows). (I-K) Loss of *Fgf10* (I), *Isl1* (J), and *Msx1* (K) expression in the dorsolateral region (arrows) of the *Lmo4*-null inner ear. The expression of *Fgf10* and *Isl1* in the cochleovestibular ganglion (CVG, asterisks) is not affected. Orientations for (A) and (B) transverse sections is indicated in (A), for (C-E) coronal sections is indicated in (C), and for (F-K) coronal sections is indicated in (F). Scale bar equals 100 μm.